The "Astropeiler Stockert Story"

Part 4: Spectral Observations
Radio Recombination Lines

Wolfgang Herrmann

1. Introduction

This is the forth part of a series of articles to introduce and describe the "Astropeiler Stockert", a radio observatory located on the Stockert Mountain in Germany. This observatory comprises a 25m dish, a 10m dish and some other smaller instruments. It is maintained and operated by a group of amateurs and is as of today the world's most capable radio observatory in the hands of amateurs.

In this series of articles I wish to describe the setup, the instrumentation and the observational results achieved.

This fifth part of the series will deal with the observation of Radio Recombination Lines.

2. Radio Recombination Lines (RRL)

The well known 21cm line from neutral hydrogen is not the only transition which can be observed in the L-band. There are other lines in this spectral range and also at other radio frequencies. However, these lines are much weaker compared to the 21 cm line.
Whereas the 21cm line originates from a hyperfine structure transition of Hydrogen atoms in the electronic ground state (n=1), Radio Recombination Lines are transitions between different electronic states of hydrogen as well as of other atoms. Transitions between electronic states are well known from the optical regime. For example, the red Balmer line of Hydrogen which is the transition between n=3 and n=2 is frequently used for solar observations. Going further up in the electronic state the next series is the "Paschen series" with transitions between n=3 and higher states. These transitions are in the infrared. As we go to higher and higher states, the energy difference of the transitions get smaller and smaller as determined by the Rydberg formula,

$$\frac{1}{\lambda} = R_H \left(\frac{1}{n_1^2} - \frac{1}{n_2^2} \right) \qquad (1)$$

where λ is the wavelength of the transition, R_H is the Rydberg constant of the hydrogen atom and n are the quantum numbers of the transition.

At some point where n_1 and n_2 are large enough, we are back in the radio regime.

Besides hydrogen, other atoms also have transitions between highly excited states which fall into the radio regime.

However, the highly excited states are normally not populated and are therefore not observable under standard conditions of interstellar matter. It requires an additional mechanism which populates these states.

3. Excitation of Radio Recombination Lines

In astronomy, such an environment which populates high electronic levels are areas where there is sufficient radiation to ionize the atoms, the so called HII regions with strong radiation from newly forming stars.
The ionized hydrogen recombines to neutral hydrogen by "catching" a free electron, and after such a recombination atoms can be in a highly excited state. This highly excited state then decays through the various electronic states by radiation. This emission is called "recombination line" as the original starting point is a recombination of an ion and an electron.

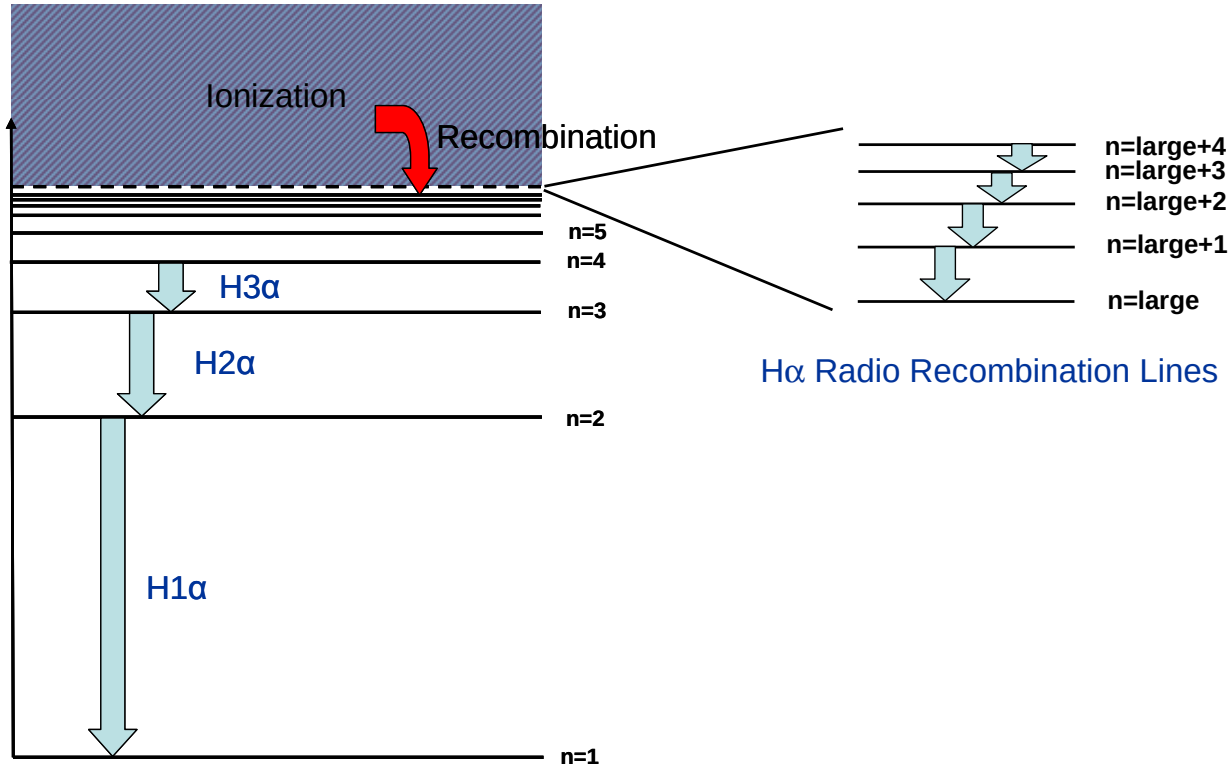

Figure 1: Energy levels of the hydrogen atom and Hα recombination lines

The same mechanism applies to other atoms as well. RRL are designated by the chemical symbol of the atom, followed by the quantum number of the lower level and a greek lettter which stands for the difference in quantum numbers for the transition (α for 1, β for 2 ....).
As an example, H165α would denote a transition between n=166 and n=165 of the hydrogen atom. H165β would denote a transition between n=167 and n=165.

4. Properties of Highly Excited Atoms

Atoms in highly excited states are called "Rydberg Atoms". These can be described in good approximation with classical physics and Bohr's atom model applies reasonably well.
Among others, the radius of the atom at an excited state of quantum number n can be calculated as:

$$r_n = n^2 \cdot a_0 \qquad (2)$$

where a_0 is the Bohr radius of $5.29 * 10^{-11}$m

In our case we will be dealing with a quantum number n in the range of 165 to 171, and in one case even as high as 241. From this it can be inferred that we are looking at atoms of an almost macroscopic radius in the range of 1.5µm or even 3.1µm.

5. A bit of history

The history of the prediction and detection of RRLs is nicely described in the book by M.A. Gordon and R.L. Sorochenko: "Radio Recombination Lines" [1]. The following section is mostly a summary of their representation.

The existence of Radio Recombination Lines was considered quite early. Van der Hulst who predicted the 21cm line also considered this possibility. He came to the conclusion, however, that Stark broadening would smear out the line so that it will be undetectable. His view was shared by other astronomers at the time.
Kardashev however came to a different conclusion in 1959 [2] using a more sophisticated model for the Stark broadening.
Encouraged by the Kardashev paper an attempt was made by Peter Mezger back in 1960 to observe the recombination lines at 11cm with our Stockert Telescope. This was unsuccessful, but he continued on the subject and was finally successful in 1965 using the 140 ft. telescope at Green Bank.
However he was not the first one to observe RRLs. The first observation reported was by Z.V. Dravskikh and A.V. Dravskikh in 1963, however this was inconclusive due to it's very poor SNR. The first observation which was convincing was by

Sorochenko and Borodzich in 1964 [3]. This observation was the H90α line at approx. 8,875 MHz.
We were honoured by Peter Mezger visiting us when we could show to him what we had achieved on his favourite subject. This was shortly before he passed away in 2014.

6. Hydrogen RRL observation approach

6.1. Observable Hα lines

The spectral range of the Stockert telescope in the 21cm region ranges from 1260 to 1440 MHz (and with some degradation up to about 1450 MHz).
In that spectral range, the following Hα RRL can be found:

H165α	1450.716 MHz
H166α	1424.734 MHz
H167α	1399.368 MHz
H168α	1374.601 MHz
H169α	1350.414 MHz
H170α	1326.792 MHz
H171α	1303.718 MHz
H172α	1281.175 MHz

The H172α line however is heavily impaired by RFI and is therefore not observable at our site. The H165α line at 1450.716 MHz is outside the "official" range and in the slope of the RF filter, but can still be observed with reduced sensitivity.

RFI in general is an issue as most RLL are outside the allocated radio astronomy band and the emission lines are quite weak. Quite a few observations were affected and therefore it was not possible to observe all lines in each and every target.

6.2. Target selection

In order to identify targets where RRLs might be observable, the literature of past observations had been scanned. Also, sifting through the Westerhout catalogue gives suggestions where to look.
As an initial target list 55 locations have been identified which are part of our ongoing observation program. Many of these locations are listed in the Westerhout catalogue.

6.3. Observational method

All observations are performed using the Fast Fourier Transform Spectrometer described earlier in this series of articles. Also, the Doppler corrections for the Local Standard of Rest reference frame (LSR) have been applied as explained in part 4 of this series. Therefore all velocities are reported with reference to LSR.

Since our receiver can cover 100 MHz at a time, two different observations are needed for each target to cover the full range, splitting up the total range in two chunks of 100 MHz each with an overlap.

Post processing of the data was done with the CLASS software package [4] using the procedure for baseline correction as described in the previous article of this series. Brightness temperature calibration, however, is somewhat uncertain. This is due to the fact that we are calibrating at the frequency of the 21cm line, and there are gain variations across the band. An effort has been made to account for these gain variations, but this is only approximate. Therefore there will be a large error margin on the reported antenna temperatures. This is particularly true for the H165α line which is already outside the RF filter main pass band.

For each observed line, a fit of a Gaussian profile has been performed in order to determine the LSR velocity, the width of the line and the (approximate) antenna temperature.

Typical integration times for an observation are 15 to 60 minutes depending on the strength of the source.

7. Hα RRL observation results

Observation of RRLs is an ongoing program at the 25m telescope. Here I report on the present state of observations, where 26 HII regions have been observed so far. 21 observations were successful, and 5 observations resulted in non-detection or questionable detection of RRL lines.

7.1. W51 region

As an example of the various observations, here is a presentation of the RRLs observed in the W51 region at RA 19:23:50, Dec 14 06 00.
W51 is a HII region with medium intensity RLL lines. i.e. neither particularly strong nor particularly weak.
In Figure 2 below, the lines H165α (at the top) through H171α (at the botton) are shown. The vertical scale is approx. 0.1 kelvin antenna temperature between ticks. All lines are shown with their velocity referenced to the local standard of rest.

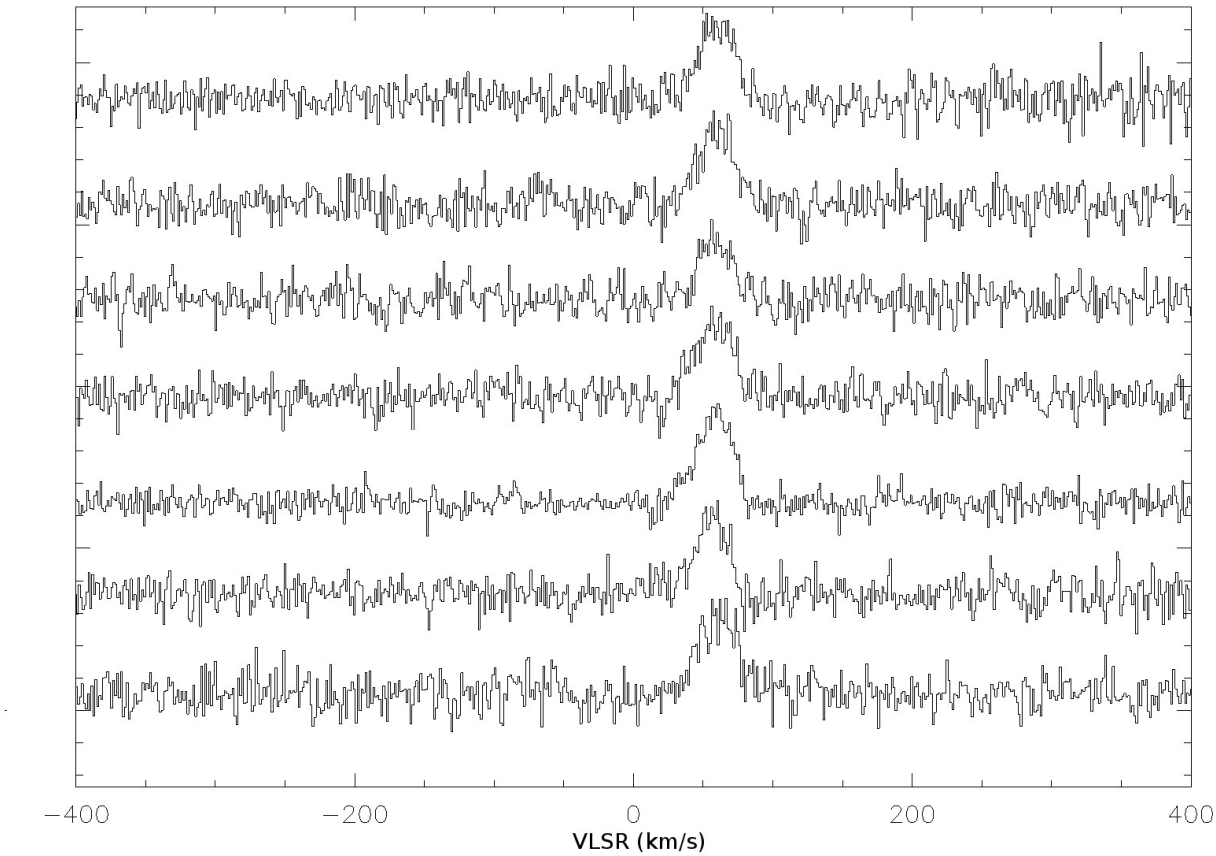

Figure 2: Hα RRLs towards W51

For further analysis, each line has been fitted with a Gaussian profile (fig.3):

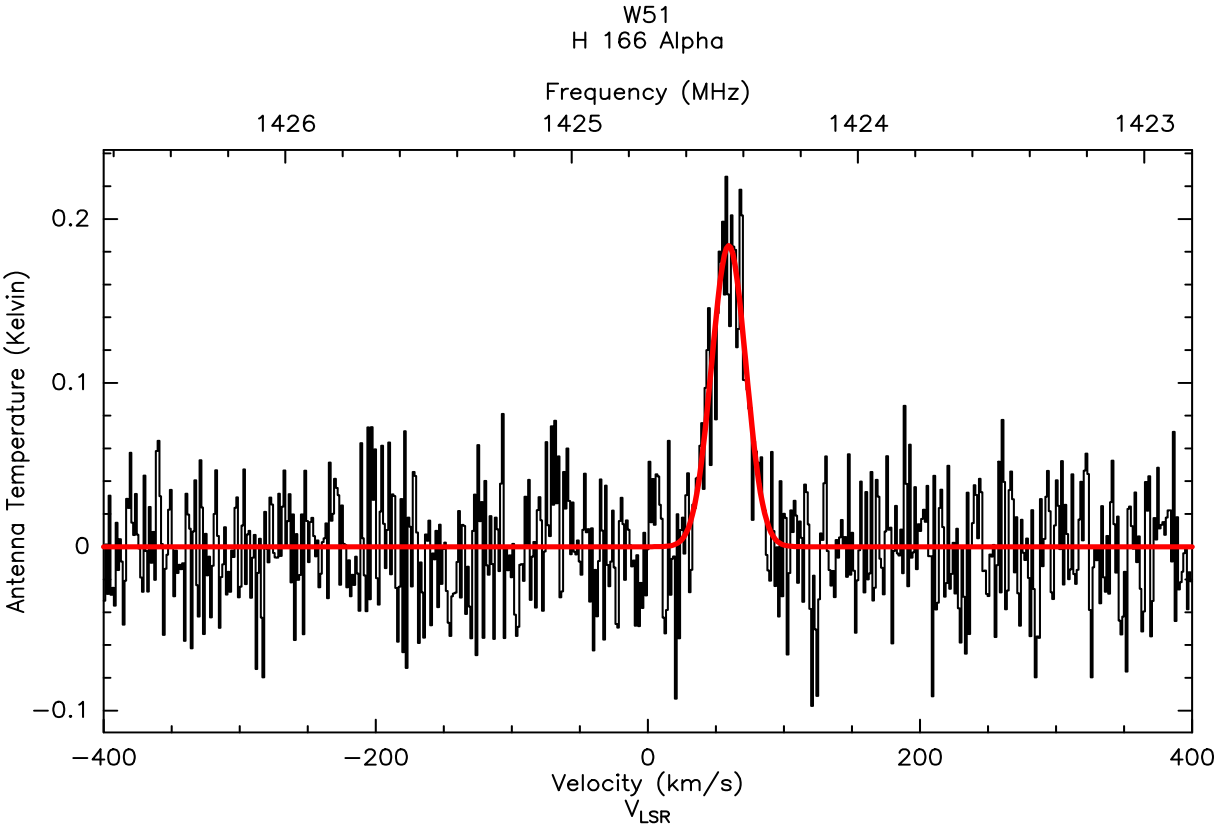

Figure 3: Gaussian fit of H166α

This procedure has been done for each observed line. The line parameters determined by this method were as follows:

Line (Rest Frequency, MHz)	T_{ant} [K]	V_{LSR} [km/s]	Line Width [km/s]
H165α (1450.716)	0.21	59.9	29.9
H166α (1424.734)	0.18	59.5	32.7
H167α (1399.368)	0.25	58.7	35.4
H168α (1374.601)	0.19	58.2	34.4
H169α (1350.414)	0.26	58.5	31.5
H170α (1326.792)	0.20	56.7	31.2
H171α (1303.718)	0.26	60.7	27.8

Table 1: Observed line parameters towards W51

7.2. Other observed regions

The total list of observed HII regions and the RRLs observed towards these regions is provided in the table 2 below.
Where no data is given, the spectral range for the line has either not yet been observed or the observations was impaired by RFI.
As an example for a weak line (0.04 K) the H166α line towards IC1848 is shown below in fig 4:

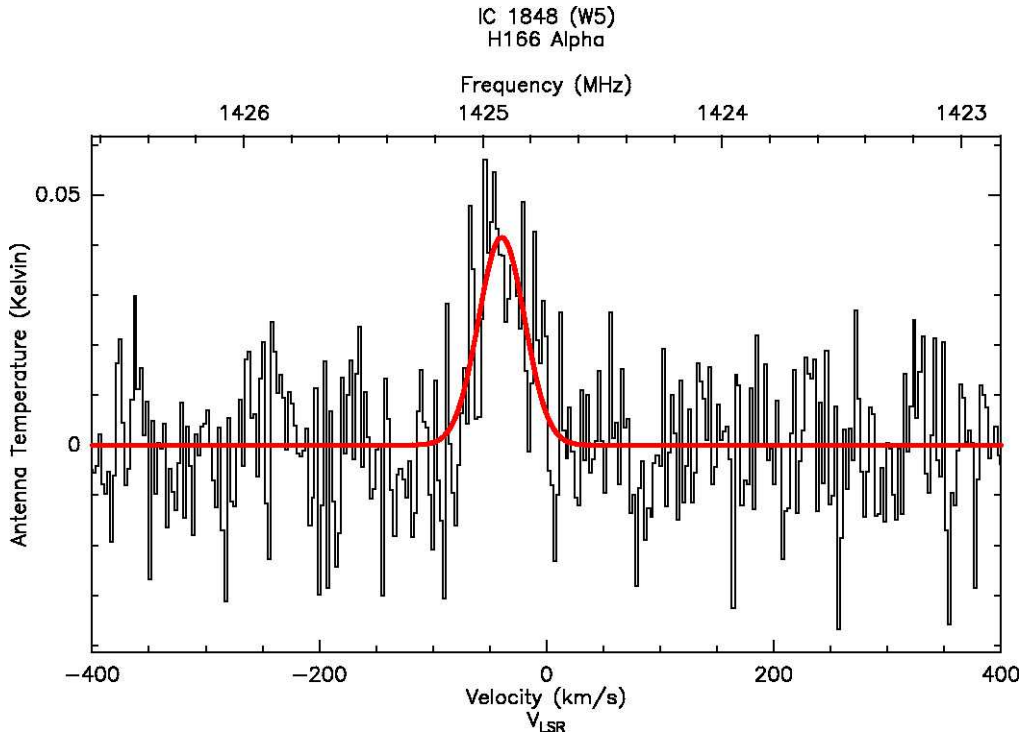

Figure 4: Weak H166α line towards IC1848

			H165Λ	H166Λ	H167Λ	H168Λ	H169Λ	H170Λ	H171Λ	
W1	**RA**	**00 01 08.58**	0,14	0,11	0,15	0,12	0,08		0,19	TA [K]
	DEC	**+67 25 17.0**	-8,4	-9,1	-10,6	-9,0	-7,4		-11,3	VLSR [km/s]
IC1795	**RA**	**02 25 43.5**	0,11	0,15	0,18					TA [K]
	DEC	**+62 06 13**	24,7	23,6	33,8					VLSR [km/s]
W3	**RA**	**02 27 04.1**	0,14	0,18	0,15					TA [K]
	DEC	**61 52 27.1**	-42,5	-43,5	-42,5					VLSR [km/s]
W4	**RA**	**02 32 42.0**	0,10	0,14	0,11					TA [K]
(Heart)	**DEC**	**+61 27 00**	-45,4	-45,5	-42,7					VLSR [km/s]
IC1848	**RA**	**02 51 06.5**	0,06	0,04						TA [K]
	DEC	**+60 24 36**	-40,1	-39,4						VLSR [km/s]
IC410	**RA**	**05 22 00.0**	0,05	0,06		0,05				TA [K]
	DEC	**+33 29 00**	-0,4	-3,5		-6,2				VLSR [km/s]
W10	**RA**	**05 35 17.3**	0,31	0,26	0,30	0,22	0,28		0,21	TA [K]
(Orion)	**DEC**	**-05 23 28**	-4,7	-4,5	-5,6	-6,6	-6,1		-6,6	VLSR [km/s]
NGC2024	**RA**	**05 41 42.7**	0,08	0,07	0,10	0,08				TA [K]
	DEC	**-01 54 44**	6,5	6,0	3,2	3,7				VLSR [km/s]
W16	**RA**	**06 31 40*.0***	0,07	0,08	0,08	0,10				TA [K]
(Rosetta)	**DEC**	**+04 57 *48***	23,5	28,5	28,7	32,5				VLSR [km/s]
Trifid	**RA**	**18 02 42.0**	0,18	0,17	0,17	0,19	0,13		0,20	TA [K]
	DEC	**-22 58 18**	17,2	15,5	15,8	15,6	14,0		14,8	VLSR [km/s]
W38	**RA**	**18 20 47.0**	0,70	0,76	0,72	0,74	0,72	0,47	0,38	TA [K]
(Omega)	**DEC**	**-16 10 18**	19,0	19,0	18,0	17,0	14,8	16,3	13,5	VLSR [km/s]
W48	**RA**	**19 01 34.5**	0,04	0,05	0,04	0,05				TA [K]
	DEC	**+01 14 16**	46,5	44,2	47,9	39,9				VLSR [km/s]
W51	**RA**	**19 23 50.0**	0,21	0,18	0,25	0,19	0,26	0,20	0,26	TA [K]
	DEC	**+14 06 00**	59,9	59,5	58,7	58,2	58,5	56,7	60,7	VLSR [km/s]
IC1318	**RA**	**20 16 48.0**	0,08	0,08	0,10					TA [K]
	DEC	**+41 57 24**	-0,3	-2,0	0,0					VLSR [km/s]
DR3	**RA**	**20 20 *24.0***	0,09	0,11	0,10	0,11			0,09	TA [K]
	DEC	**+40 43 *00***	-5,0	-7,9	-2,7	-1,9			1,0	VLSR [km/s]
DR13	**RA**	**20 31 00**	0,13	0,15	0,14	0,15			0,15	TA [K]
	DEC	**+38 58 12**	-4,8	-3,5	-2,9	-2,1			-3,4	VLSR [km/s]
W71	**RA**	**20 35 0*0.0***	0,10	0,09	0,11	0,07	0,09	0,12	0,10	TA [K]
	DEC	**+47 02 *00***	-4,7	-6,6	-6,3	1,4	-2,8	3,8	-4,0	VLSR [km/s]
W75	**RA**	**20 39 01.6**	0,11	0,23	0,29	0,26			0,24	TA [K]
(DR23)	**DEC**	**+42 22 47**	6,5	5,3	6,9	6,8			5,8	VLSR [km/s]
DR22	**RA**	**20 39 16.67**	0,04	0,13	0,13	0,11			0,12	TA [K]
	DEC	**+41 18 44.7**	23,2	29,7	26,6	28,4			28,4	VLSR [km/s]
W80	**RA**	**20 58 *47.0***	0,15	0,13	0,10	0,15				TA [K]
(North America)	**DEC**	**+44 19 *48***	-1,1	-1,1	-1,7	-1,8				VLSR [km/s]
NGC7380	**RA**	**22 47 21*.0***		0,04	0,06					TA [K]
	DEC	**+58 07 *54***		-49,7	-43,8					VLSR [km/s]

Table 2: Observed antenna temperature (TA) and velocity (VLSR) towards various HII regions

8. Deep observation of RRLs in the Orion nebula

Besides the HII regions mentioned above, specific deep (long integration times) observations have been performed towards the Orion Nebula (aka M42, W10, 3C145). This area has comparatively strong recombination lines and allows observation of additional RRLs.

8.1. Carbon Recombination Lines

Besides the hydrogen recombination lines, RRLs from carbon can be observed in some HII regions where the formation of RRLs is strong. One of these areas is the Orion nebula.
Below is a spectrum showing both the H166α and the C166α from this area (fig 5:):

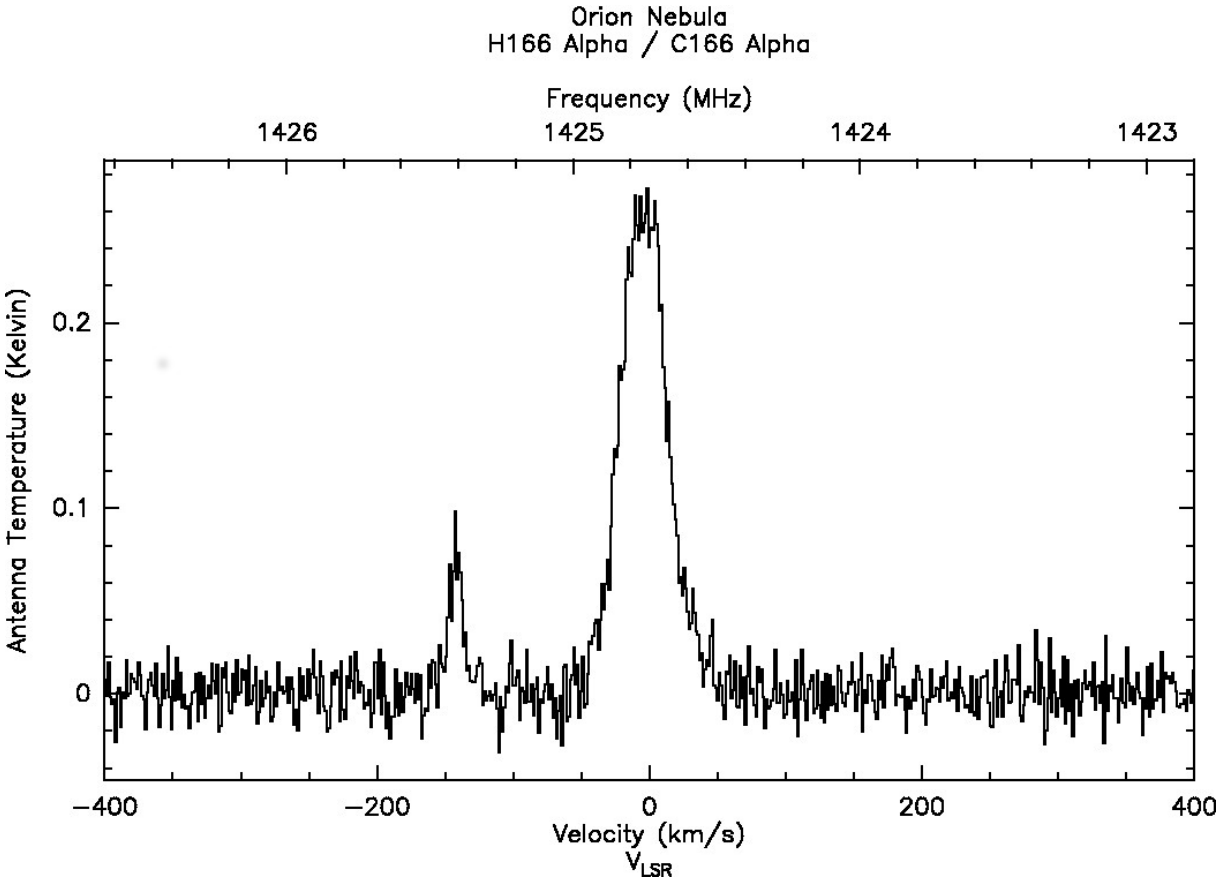

Figure 5: Spectrum of H166α and C166α

The carbon line is shifted to higher frequencies due to the heavier nucleus. For the same reason, the line is much narrower as the Doppler broadening is less.

From this spectrum, the velocity of the carbon line has been determined to be 7.9 km/s. This is different from the velocity of the hydrogen line which is around -6 km/s. This seems surprising, as one would expect the same velocity from one HII region. However, the observation is consistent with other observations of carbon

recombination lines in the Orion nebula [5], [14]. The explanation for this difference is that the hydrogen and carbon RRLs are originating from different areas in the nebula with different physical conditions.

8.2. Observation of higher order transitions: Hβ and Hγ RRLs

Radio recombination lines do not only originate from transitions between neighbouring levels with $\Delta n = 1$. Also higher order transitions can be observed, albeit with less intensity. In case of the Orion nebula we were able to observe transitions with $\Delta n = 2$, i.e. Hβ lines. In this case, n has to be even higher in order to fall within the frequency range of the receiver.
Both the H 212β and the H 208β were observed, the latter is shown below in figure 6 at 1440.720 MHz:

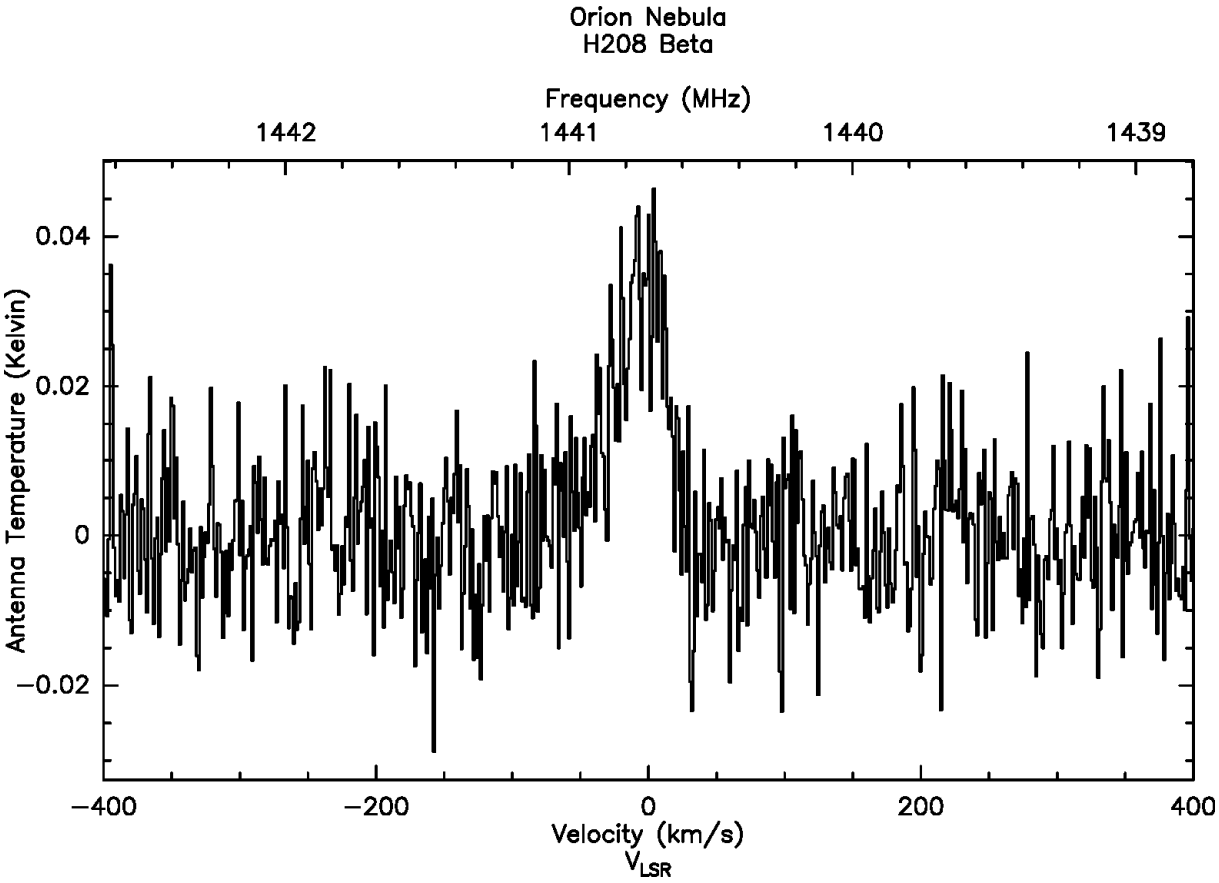

Figure 6: Observation of the H 208β line

Other Hβ lines which should be observable in principle were affected by RFI. At antenna temperatures in the order of 20 mKelvin we are going to our sensitivity limit and even a tiny amount of RFI makes observations unusable or questionable.

Really stretching the sensitivity limit was the observation of the $\Delta n = 3$ line H 241γ. In order to improve the SNR, the spectral resolution was reduced from about 6.1 kHz to

12.2 kHz by re-binning the data (fig. 7). The rest frequency of this line is 1383.528 MHz.

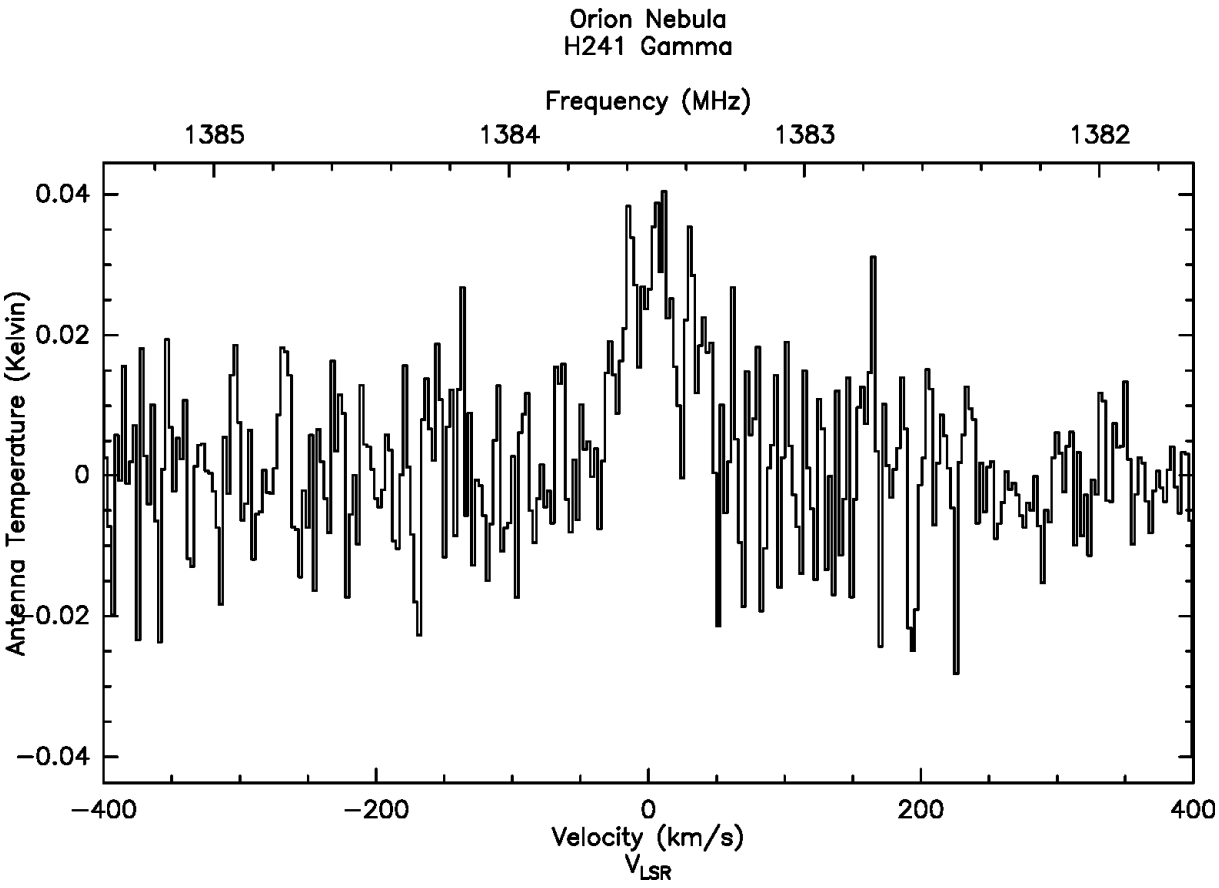

Figure 7: Observation of the H 241γ line

In reviewing the literature, I could find just one publication which reports on the observation of a Hnγ line towards Orion at L-Band frequencies [6]. This was the H225γ line at 1667 MHz. I therefore believe that the observation reported here may actually be the first time that the H241γ line has been observed.

9. Determining electron temperature in HII regions from RRL observations

9.1. Background

Observation of Radio Recombination Lines offer an interesting feature: By measuring the ratio between the line intensity and the intensity of the continuum radiation along with the width of the line it is possible to determine the electron temperature of the HII region.

The theory behind this is a bit involved. I am referring the interested reader to [7] and [8] for a more detailed explanation.

However, for a basic understanding it may suffice to know that both the line intensity of RRLs and the continuum radiation are dependent on the electron temperature and the frequency, but with different exponents.

This allows to determine the electron temperature as:

$$T_e^{1.15} = \frac{T_C}{T_L} \cdot \frac{1}{\Delta V} \cdot \frac{6.985 \cdot 10^3}{a(T_e, \nu)} \cdot \nu^{1.1} \cdot \frac{1}{1 - 0.08} \qquad (3)$$

where T_C/T_L is the ratio of the continuum to line intensity, ΔV is the line width in km/sec, υ is the line frequency in GHz and T_e is the electron temperature in kelvin. a(Te, υ) is a function introduced by Mezger and Henderson [6] which is almost 1 for most of the combinations of electron temperature and frequency. In our case a value of 0.98 has been used. The factor 1+0.08 reflects the abundance of Helium (8% in the case of Orion).

9.2. Observational approach

As can be seen from equation (3) there are three parameters which need to be measured: The continuum intensity, the line intensity and the line width. Fortunately, the measurement is not sensitive to calibration errors as only the ratio of the continuum and line intensity is required. Therefore there is no need for absolute calibration.

In order to precisely determine the line intensity and line width, long integration times are required. However, this impacts the accuracy of the continuum intensity measurement: As the telescope moves during the observation, the amount of thermal pickup changes slightly.
Therefore the observation was organized as follows:
Initially, an observation was done for 5 minutes pointing at a location close to Orion but "off target" to determine the system noise background. Then a 30 min observation was performed to determine both the line intensity and the continuum intensity including system noise background. Then another 5 min observation in an "off target" position was done in order to determine changes in the system noise background.
This procedure was repeated several times during an observation session.

The average of the two off target observations was subtracted from the on target continuum signal in order to determine the continuum intensity from Orion.
The line intensity and width was determined by fitting a Gaussian profile to the line data as explained above.

9.3. Observational results and discussion

Three observation sessions were performed with the following results:

Observation #	$T_{continuum}$ [K]	T_{line} [K]	Line Width [km/s]	T_e [K]
1	33.2	0.269	36.5	8481
2	35.15	0.251	40.0	8741
3	38.21	0.267	39.7	8971
Average				**8731**

Table 3: Results of measurements of the Electron temperature in the Orion Nebula

In order to do a sanity check on the results, they were compared with published results. There is quite a bit of literature from numerous observations at various recombination lines. Also, some observations have sufficient spatial resolution so that it could be demonstrated that the electron temperature varies over different regions of the Orion nebula, and several electron temperatures are given in a single publication. The data from the publications [9] through [19] has been collected and grouped in a histogram showing how frequently which temperature range is observed (see Fig. 8):

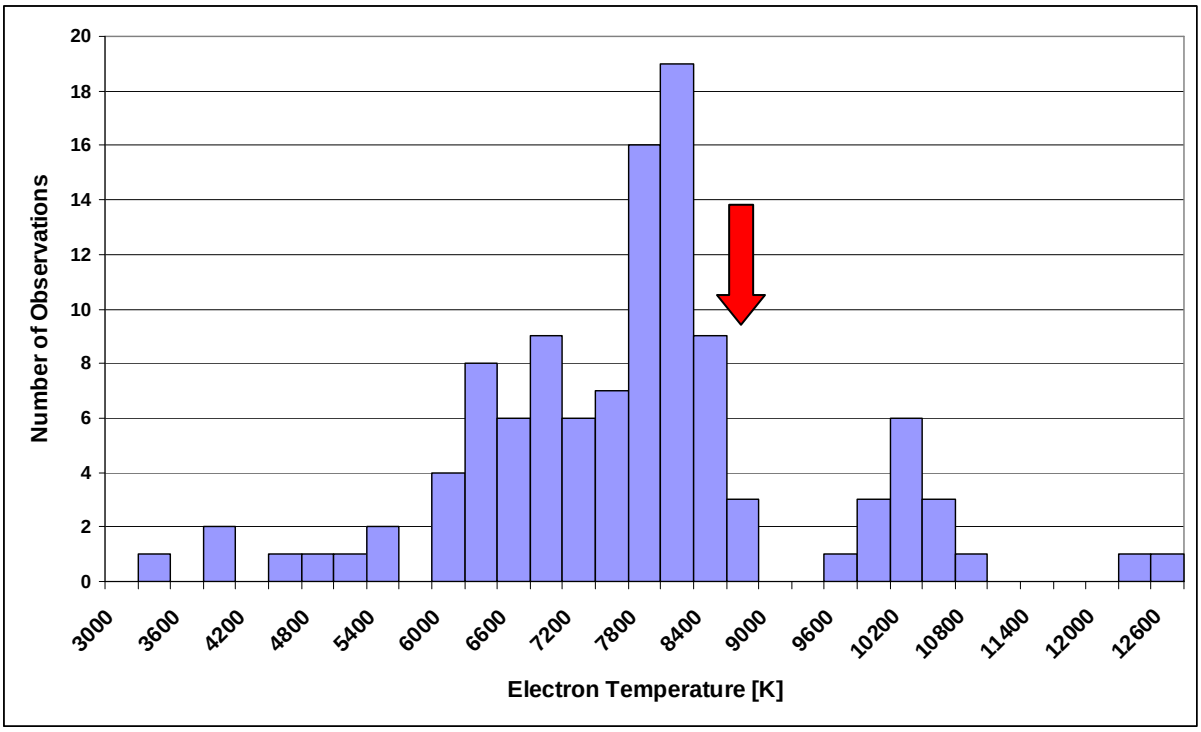

Figure 8: Histogram of observations from literature compared to own observation

The red arrows shows where this observation is positioned compared to other observations. It seems a bit on the high side, but still well within the range of previous measurements.

10. Summary and conclusion

The observation of Radio Recombination Lines originating from various HII regions is reported. The results presented are from an ongoing observation program in the 1450 to 1260 MHz spectral range with the Astropeiler Stockert 25m telescope where 26 regions have been observed so far. 21 of these regions show emissions from RRLs, 5 were non-detections.
RRLs can be used to determine the physical environment in a HII regions, such as the electron temperature. This has been demonstrated for the Orion nebula.

RRLs are weak. The strongest emissions are a factor of 100 less than the typical 1420 MHz line from neutral hydrogen. Therefore, the observation with "typical" amateur instruments of 3m diameter may not be possible. However, the stronger lines such as from the Orion nebula may be within the realm of possibilities for larger amateur instruments in the range of 8m and above.

The observation program will continue by complementing the data with more observations in the already observed regions as well as observing additional regions.

References:

[1] M.A. Gordon and R.L. Sorochenko, Radio Recombination Lines, Their Physics and Astronomical Applications; Astrophysics and Space Science Library, Springer 2009, ISBN 978-0-387-09604-9
[2] N.S. Kardashev, Astron. Zh, 36, 383 (1959). English translation: Sov. Astron. AJ 3:813 (1960)
[3] R.L. Sorochenko, E.V. Borodzich, Paper presented at the XII assembly of the IAU, Hamburg (1964); Trans. IAU XIIB, (1966)
[4] https://www.iram.fr/IRAMFR/GILDAS/
[5] F. Wyrowski, P. Schilke, P. Hofner, C.M. Walmsley, Ap J 487, L171-L174 (1997)
[6] D.R.W. Williams, Astrophys. Lett. 1, 59-63 (1967)
[7] M.I.R Alves, PhD Thesis, Univ. of Manchester (2011), available at userpages.irap.omp.eu/~malves/SiteIRAP/Publications_files/Thesis_finalv_sub.pdf
[8] P.G. Mezger, A.P. Henderson, Ap J 147, 471 (1967)
[9] P.G. Mezger, B. Höglund, Ap J 147, 490 (1967)
[10] N.H. Dieter, Ap J 150, 435 (1967)
[11] M.A. Gordon, M.L. Meeks, Ap J 152, 417 (1968)
[12] E.C. Reifenstein, T.L. Wilson, B.F. Burke, A&A 4, 357-377 (1970)
[13] R.M. Hjellming and M.A. Gordon, Ap J 164, 47-60 (1971)
[14] F.J. Lockman, R.L. Brown, Ap J 201, 134-150 (1975)
[15] E.J. Chaisson, M.A. Dopita, A&A 56, 385 (1976)
[16] T. Pauls, ´T.L. Wilson, A&A 60, L31-L33 (1977)
[17] V. Pankonin, C.M. Walmsley, M. Harwit, A&A 75, 34-43 (1979)
[18] S.M. Lichten, L.F. Rodriguez, E.J. Chaisson, Ap J 229, 524-532 (1979)
[19] D. Hoang-Binh, P. Encrenaz, R.A. Linke, A&A L19-L21 (1985)